Experimental Comparison of Adaptive Optics Algorithms in 10-Gb/s Multimode Fiber Systems

Rahul Alex Panicker, Alan Pak Tao Lau, Jeffrey P. Wilde, and Joseph M. Kahn, *Fellow, IEEE*

***Abstract*—We experimentally compare various adaptive algorithms that use a spatial light modulator (SLM) to compensate modal dispersion in 50-μm graded-index multimode fibers. We show that continuous-phase sequential coordinate ascent (CPSCA) gives better bit-error-ratio performance than 2- or 4-phase sequential coordinate ascent, in concordance with simulations in [10]. We then evaluate the bandwidth characteristics of CPSCA, and show that a single SLM is able to simultaneously compensate the modal dispersion in up to 9 wavelength-division-multiplexed 10-Gb/s channels, spaced by 50 GHz, over a total bandwidth of 450 GHz. We also show that CPSCA is able to compensate for modal dispersion in fibers up to 2.2 km long, even in the presence of midspan connector offsets up to 4 μm (simulated in experiment by offset splices). A known non-adaptive launching technique using a fusion-spliced single-mode-to-multimode patchcord is shown to fail under these conditions.**

***Index Terms*—Adaptive optics, algorithms, optical fiber dispersion, spatial light modulators.**

I. Introduction

MULTIMODE FIBER (MMF) is the dominant type of fiber used for data communications in current local-area networks. In attempting to achieve higher signaling rates, the dominant limiting factor is the inter-symbol interference (ISI) caused by modal dispersion [1]. Light propagates in a MMF in modes, with each mode propagating at its group velocity. The set of modes excited depends on launch conditions at the input of the fiber, and on mode coupling within the fiber. Thus, a pulse of light that excites multiple modes in the fiber arrives as several pulses at the output of the fiber, a phenomenon known as modal dispersion.

In describing modal dispersion, the relevant modes are typically not the modes of an ideal fiber, which we refer to as ideal modes (IM). Bends and imperfections in the refractive index profile cause coupling between IMs. This means that a pulse launched into an IM will be received as a sequence of pulses. However, it has been shown [2] that there exists a complete set of orthonormal modes, called principal modes (PMs), such that a pulse launched into a PM at the input of the fiber emerges as a single pulse at the output, even in the presence of mode coupling. PMs in MMFs with mode coupling are analogous to principal states of polarization (PSPs) in single-mode fibers (SMF) with polarization-mode dispersion.

In the past, electrical equalization [3], [4] has been used to mitigate ISI caused by modal dispersion. However, this can lead to noise enhancement, and, therefore, degradation of achievable bit-error ratio (BER) [5].

As an alternative to electrical equalization, the use of adaptive optical compensation was proposed in [6]. This involves shaping the spatial profile of the electric field at the input end of the fiber using a spatial light modulator (SLM) to excite only desired PMs. An SLM is a two-dimensional array of pixels, capable of modifying the local phase and/or amplitude of an incident electric field. This technique leads to no noise enhancement, and compares favorably with electrical equalization techniques, such as the optimal maximum-likelihood sequence detection (MLSD) [7]. Experiments [8], [9] have shown that this approach is capable of achieving multi-kilometer transmission at bit rates of 10 and 100 Gb/s.

A comprehensive theoretical framework for analyzing adaptive optical compensation was developed in [7]. It was shown that minimizing ISI by changing the SLM settings can be posed as a convex optimization problem. In particular, maximizing eye opening, subject to constraints on the SLM, was cast as a second-order cone program. Adaptive algorithms for optimizing the SLM in real time were proposed in [10]. The continuous-phase sequential coordinate ascent (CPSCA) algorithm was shown to achieve the best performance in simulation. In this paper, we demonstrate the efficacy of this algorithm experimentally, and compare its performance with that of 2-phase sequential coordinate ascent (2PSCA), and 4-phase sequential coordinate ascent (4PSCA).

The remainder of the paper is organized as follows. In Section II, we describe the experimental setup used. In Section III, we give theoretical background for analysis of the system. In Section IV, we compare the performance of 2PSCA, 4PSCA, and CPSCA, with various fiber configurations, and show that CPSCA gives better BER performance than 2PSCA or 4PSCA, in concordance with simulations in [10]. We then evaluate the bandwidth characteristics of CPSCA, showing that a single SLM is able to simultaneously compensate the modal dispersion of several wavelength-division-muliplexed (WDM) channels. We also show that CPSCA is able to compensate

Manuscript received January 05, 2008; revised April 29, 2008. First published November 13, 2009; current version published December 02, 2009. This work was supported in part by the National Science Foundation under Grant ECCS-0700899.

R. A. Panicker was with the Department of Electrical Engineering, Stanford University, Stanford, CA 94305 USA. He is now with Embrace, Richmond Town, Bangalore 560025, India (e-mail: rahul@embraceglobal.org).

A. P. T. Lau was with the Department of Electrical Engineering, Stanford University, Stanford, CA 94305 USA. He is now with the Department of Electrical Engineering, Hong Kong Polytechnic University, Hung Hom, Kowloon, Hong Kong (e-mail: eeaptlau@polyu.edu.hk).

J. P. Wilde and J. M. Kahn are with the Department of Electrical Engineering, Stanford University, Stanford, CA 94305 USA (e-mail: jpwilde@stanford.edu, jmk@ee.stanford.edu).

Digital Object Identifier 10.1109/JLT.2009.2036683

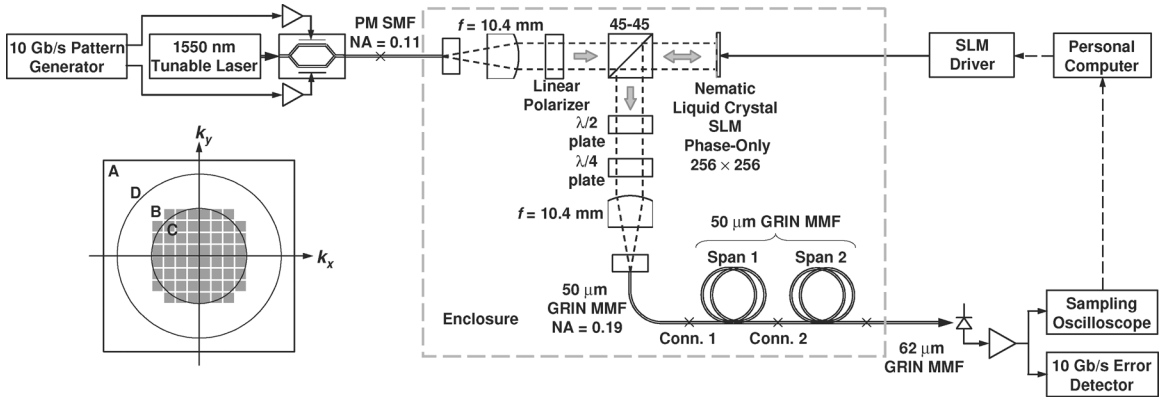

Fig. 1. Experimental setup. Inset: spatial light modulator (SLM) in Fourier plane of the input face of multimode fiber (MMF). A: boundary of SLM active region. B: Block structure of SLM pattern. C: Circle enclosing 95% of power of beam incident on SLM, corresponding to a numerical aperture (NA) of 0.11 at the MMF input. D: Circle corresponding to the MMF NA of 0.19.

for modal dispersion even in the presence of midspan offset interconnections.

II. Experimental Setup

The experimental system is shown in Fig. 1. A C-band laser can be tuned to a comb of 100 channels, spaced by 50 GHz, covering a 5.0 THz bandwidth over the 1527–1567 nm wavelength range. A Mach–Zehnder modulator encodes a chirp-free 10 Gb/s non-return-to-zero signal having $+6$ dBm average power, which is output into a polarization-maintaining SMF (PM-SMF) having a numerical aperture (NA) of 0.11. The PM-SMF output, in the LP_{01} mode, is collimated by an $f = 10.4$ mm plano-convex lens, passed through a polarizer, and used to illuminate a liquid crystal SLM. The linear polarizer aligns the PM-SMF output to the linear state of polarization (SOP) required at the SLM.

The nematic liquid crystal, phase-only SLM has 256×256 pixels, each $18\ \mu\text{m} \times 18\ \mu\text{m}$ in size, each independently controllable with 5–6 bit resolution over the range 0–2π, with switching times of 100 ms $(0 \leftrightarrow 2\pi, 10\% \leftrightarrow 90\%)$. After reflecting from the SLM and passing through a 45%–45% polarization-independent beam splitter, the beam is coupled into a MMF using an $f = 10.4$ mm plano-convex lens, resulting in a launched NA of 0.11. The beam spot is nominally center-launched to excite lower-order modes preferentially. A half-wave plate and a quarter-wave plate allow the launched signal to be adjusted to an arbitrary SOP. The free-space optical system has a loss of about 8.5 dB. So, an average power of about -2.5 dBm is launched (for a blank SLM pattern).

Test fibers are spooled, plastic-jacketed, standard 50-μm graded-index MMF, having power-law index profiles with exponent between 2.00 and 2.03, and NA of 0.19 at C-band wavelengths. These are indicated in Fig. 1 as "Span 1" and "Span 2". In order to simulate connector offsets in deployed systems, patchcords with offset fusion splices of 0, 2 or 4 μm are inserted before and/or between the test fibers. These are indicated in Fig. 1 as "Conn. 1" and "Conn. 2". The test fiber output is connected via a 62.5-μm MMF pigtail to a commercial receiver comprising an InGaAs *p-i-n* photodiode and transimpedance preamplifier, and having d.c.-9.5 GHz bandwidth (at -3 dB). The sensitivity and overload power are -20 dBm and $+2$ dBm, respectively, both at 10^{-10} BER.

Receiver electrical output waveforms are acquired by a sampling oscilloscope and sent via a GPIB interface to a personal computer, which estimates ISI, executes an adaptive algorithm, and controls the SLM. The SLM, situated in the Fourier plane of the MMF input, performs spatial signal processing. The SLM surface is depicted in the inset of Fig. 1. Coordinates on the SLM are denoted by spatial frequencies. "A" denotes the boundary of the 256×256-pixel active region. To reduce both the complexity and the adaptation time, square blocks comprising 16×16 pixels are utilized. The phase of each block is adjusted during adaptation. A set of 60 such blocks is used, denoted by "B". This set covers a circle enclosing 95% of the energy of the incident LP_{01} mode of the PM-SMF, denoted by "C", which corresponds to an NA of 0.11 in the MMF. The circle "D" denotes the MMF NA of 0.19.

III. Analytical Characterization

In this section, we provide theoretical background for analyzing our adaptive-optics system. We first give an expression for the impulse response of the system in terms of the SLM settings and the mode fields of the PMs of the fiber. Next, we give an expression for the objective function, i.e., the vertical eye opening, which we wish to maximize. We then give a procedure for estimating the objective function when the eye is closed. Finally, we give a brief explanation of the adaptive algorithms that are being experimentally compared.

A. Impulse Response

With a given SLM setting, the electric field of a time-domain pulse entering the MMF has a certain spatial profile. This in turn governs the set of PMs excited, and the distribution of energy across the PMs. Since each PM propagates with a well-defined group delay, we obtain a sequence of pulses at the output. For a unit impulse at the input, this sequence of output impulses forms the impulse response. Note that the impulse response referred to here is an intensity impulse response. Thus, the impulse response of the system is a function of the SLM settings.

A detailed derivation was presented in [7]. Here, we reproduce some of the key results

$$h(t) = e^{-\alpha l} \sum_{i=1}^{2M} \left| \int \left[\vec{\mathbf{E}}_{\text{fiberIn}}(x,y) \times \vec{\mathbf{H}}^{*}_{\text{PM},i}(x,y) \right] \cdot \hat{z}\, dx\, dy \right|^2 \delta(t - \tau_i), \quad (1)$$

where α is the fiber loss coefficient (approximated as mode-independent), l is the fiber length, $2M$ is the number of propagating PMs in both polarizations, $\vec{\mathbf{E}}_{\text{fiberIn}}(x,y)$ is the electric field at the input face of the fiber, $\vec{\mathbf{H}}_{\text{PM},i}(x,y)$ is the normalized magnetic field corresponding to the ith input PM, and τ_i is the group delay of the ith PM. $\vec{\mathbf{E}}_{\text{fiberIn}}(x,y)$ is a function of the SLM pixel reflectances, an exact expression for which is given in [7]. This leads to a final expression of the impulse response of the following form:

$$h(t) = \mathbf{v}^H \left[\sum_{i=1}^{2M} \mathbf{u}_i \mathbf{u}_i^H \delta(t - \tau_i) \right] \mathbf{v} \quad (2)$$

where $\mathbf{v} = [v_1\, v_2 \ldots v_N]^T$, $v_j \in \mathbb{C}$ is the reflectance of the jth SLM block, N is the number of SLM blocks, and $\mathbf{u}_i \in \mathbb{C}^N$, $i = 1, \ldots, 2M$ are vectors that capture the spatial structure of the $2M$ PMs [7]. Note that the intensity impulse response is a quadratic function of the SLM reflectances.

B. Objective Function

The pulse response of the system was shown [7] to be

$$\begin{aligned} g(t) &= h(t) * q(t) \\ &= \mathbf{v}^H \left[\sum_{m=1}^{2M} \mathbf{u}_m \mathbf{u}_m^H q(t - \tau_m) \right] \mathbf{v} \end{aligned} \quad (3)$$

where $q(t) = p(t) * r(t)$, with $p(t)$ being the transmit intensity pulse, and $r(t)$ the receiver impulse response. It was also shown that minimization of ISI is equivalent to maximization of the vertical eye opening in the eye diagram generated by the above pulse response. The eye opening is given by

$$F(g(nT; t_0)) = g(0; t_0) - \sum_{n \neq 0} g(nT; t_0) \quad (4)$$

where T is the bit duration, t_0 is an initial sampling offset, and n is an integer, with $n = 0$ corresponding to the desired peak. F is directly proportional to the eye opening, with $F < 0$ when the eye is closed, and $F > 0$ when the eye is open. Minimization of ISI was shown to be equivalent to maximization of F.

It was also shown in [7] that F can be simplified to the form $F = \mathbf{v}^H \mathbf{P} \mathbf{v}$, where $\mathbf{P} \in \mathbb{C}^{N \times N}$ is a Hermitian matrix, with one positive, and $N - 1$ non-positive eigenvalues. $\mathbf{P}$ characterizes the system. We note that in real fiber systems, $\mathbf{P}$ is not known explicitly, since it captures the details of the mode-coupling and the optical system, and depends on the exact refractive profile, fiber bends and twists, etc. Hence, maximization of F requires an adaptive algorithm.

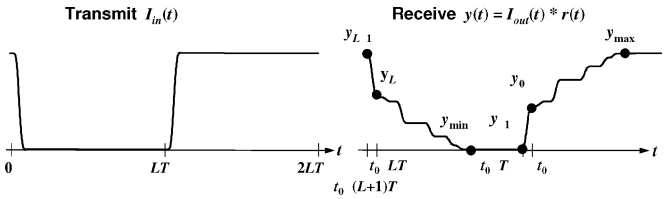

Fig. 2. Estimation of the objective function using six samples from the response to a step training sequence.

C. Estimating the Objective Function

If we can observe $\mathbf{v}^H \mathbf{P} \mathbf{v}$ for every SLM setting $\mathbf{v}$, then we can find the optimal solution without explicit knowledge of $\mathbf{P}$. Since $\mathbf{v}^H \mathbf{P} \mathbf{v}$ is the eye opening, it can be measured directly when the eye is open.

While it may appear from (4) that estimating F when the eye is closed requires many samples of the impulse response, in practice, it can be estimated from a few samples of the step response. For example, in [8], the following procedure was used. When the eye is closed, a periodic training sequence comprising a long string of 0-bits followed by an equal number of 1-bits is transmitted, as shown in Fig. 2. Here, L is number of 0-bits (or 1-bits) in the sequence. The largest positive and negative excursions of the received waveform over any interval of duration T is used to estimate $g(0; t_0)$, and the total excursion of the received waveform is used to estimate $\sum g(nT; t_0)$. F is then estimated as

$$F = (y_0 - y_{-1}) + (y_{L-1} - y_L) - (y_{\max} - y_{\min}).$$

In [8], a value of $L = 64$ was used. When the eye is open, the eye opening itself may be used as an estimate of F.

D. Adaptive Algorithms: CPSCA, 4PSCA, and 2PSCA

Algorithm 1 Continuous-Phase Sequential Coordinate Ascent (CPSCA)

1: $v_i := 1, \quad i = 1, \ldots, N.$
2: $i := 1$
3: **repeat**
4: **for** $m = 1$ to 3 **do**
5: $v_i := \exp(j2\pi(m-1)/(3))$
6: Estimate F_m
7: **end for**
8: $b := \frac{(2F_1 - F_2 - F_3) + j\sqrt{3}(F_2 - F_1)}{3}$
9: $v_{\text{opt}} := \exp(j \arg(b))$
10: $v_i := v_{\text{opt}}$
11: $i := (i) \bmod (N) + 1$
12: **until** Termination

CPSCA (Algorithm 1) was introduced in [10] as an algorithm for optimizing the SLM. A single SLM block is selected, and its

phase is optimized to maximize the objective function, i.e., the eye opening. Three estimations of the eye opening are required to optimize a single SLM block. The objective function is estimated using the procedure described in Section III.C. Next, another SLM block is selected, and the process is repeated. The objective function was shown to converge to a value very close to the global maximum.

Maximizing the objective function with respect to the phase of a single SLM block is in itself an optimization problem. It was shown in [10] that

$$F = \Re\{b^* \exp(j\phi_i)\} + d \tag{5}$$

where $\phi_i = \arg(v_i)$, $b \in \mathbb{C}$, and $d \in \mathbb{R}$. The optimal ϕ_i is given by $\arg(b)$, where b is estimated using measurements of F at three different values of ϕ_i.

In 4PSCA, a single SLM block is chosen, and its phase is optimized over the set $\{0, \pi/2, \pi, 3\pi/2\}$ to maximize the eye opening. Next, another SLM block is chosen, and the process is repeated. 2PSCA, which is the algorithm used in [8], is similar to 4PSCA, except that the phase of an SLM block is optimized over the set $\{0, \pi\}$. It is to be noted that, to optimize a single SLM block, CPSCA requires three SLM block flips and estimations of the objective function, 4PSCA requires four, and 2PSCA requires two.

In the experimental setup described in this paper, each time an SLM block is changed, the received waveform is acquired by the sampling oscilloscope for estimation of $F(g(nT; t_0))$. Eight samples per bit interval are taken to obtain sufficient resolution in choosing t_0, and four acquisitions of the waveform are averaged to reduce thermal and quantization noises. In order to estimate F using the procedure described in Section III.C, we use the periodic step training sequence with $L = 64$. A single estimation of F requires about 0.9 s, which is dominated by waveform sampling and GPIB interface latency. In a single iteration of the adaptive algorithm, the 60 SLM blocks are optimized one-by-one, proceeding outward from the center in concentric rings, which takes about 3 minutes in the current setup. With a faster SLM based on microelectromechanical systems, switching time for the SLM could be reduced to 10 μs [11]. The use of dedicated hardware can reduce the time required for estimation of the objective function F to 10 μs. Thus, assuming a round-trip propagation time of 10 μs, the time required for a single SLM block flip could be reduced to 30 μs. Therefore, the time required for a single iteration of CPSCA, corresponding to 180 block flips, could be reduced to about 5.4 ms.

IV. Results

A. Comparison of CPSCA, 4PSCA, and 2PSCA

We compare the performance of CPSCA, 4PSCA, and 2PSCA, for various fiber configurations, and show that CPSCA gives better BER performance than 4PSCA or 2PSCA. A fiber configuration involves a combination of offset patchcords and segments of straight fiber, and its configuration is indicated as "a μm/b m" or "a μm/b m/c μm/d m". In Fig. 1, a and c are the offsets of the patchcords indicated as "Conn. 1" and "Conn. 2" respectively, while b and d are the lengths of "Span 1" and "Span 2" respectively. So, for e.g., 2 μm/2200 m indicates a 2-μm offset patchcord followed by 2200 m of fiber, and 2 μm/500 m/2 μm/500 m indicates a 2-μm offset patchcord, 500 m of fiber, another 2-μm offset patchcord, and 500 m of fiber. System BER performance is measured at a bit rate of 10 Gb/s using a $2^{31} - 1$ psuedorandom binary sequence, and a gating period of 3 s.

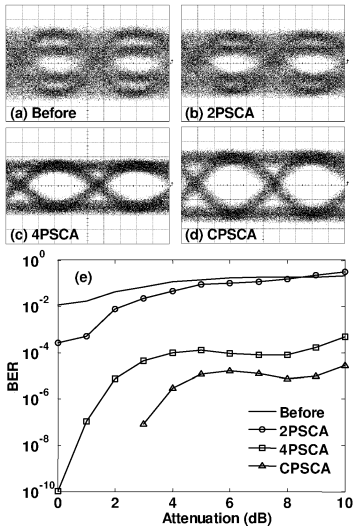

Fig. 3. Fiber configuration 2 μm/2200 m: eye diagrams (a) before adaptation, (b) after 2PSCA, (c) after 4PSCA, (d) after CPSCA; (e) BER versus attenuation.

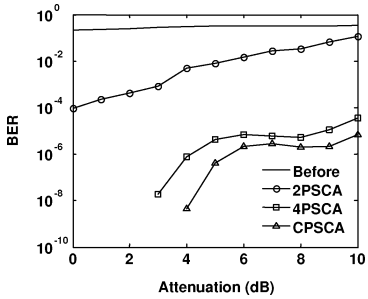

Fig. 4. Fiber configuration 4 μm/2200 m: BER versus attenuation before adaptation, and after CPSCA, 4PSCA, and 2PSCA.

Fig. 3 shows performance of various algorithms for a 2 μm/2200 m configuration. The BER curves indicate that CPSCA gives better BER performance than 2PSCA or 4PSCA. The eye opening after CPSCA is also visibly larger than after 2PSCA or 4PSCA. Since the mode coupling in the fiber changes with time due to change in temperature, etc., the experiment was repeated multiple times, and with various launch polarizations. The set of figures presented here is a typical realization.

Figs. 4–6 show similar comparisons for 4 μm/2200 m, 2 μm/1000 m, and 4 μm/1000 m configurations respectively. In all these cases, CPSCA gives better BER performance than 2PSCA and 4PSCA.

These experiments clearly demonstrate that CPSCA consistently gives better BER performance than both 4PSCA and 2PSCA.

B. Further Evaluation of CPSCA

Since it was shown in Section IV.A that CPSCA gives better BER performance than 4PSCA and 2PSCA, in this section, we

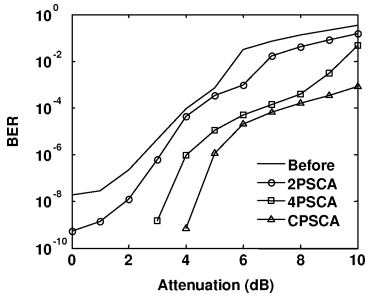

Fig. 5. Fiber configuration 2 μm/1000 m: BER versus attenuation before adaptation, and after CPSCA, 4PSCA, and 2PSCA.

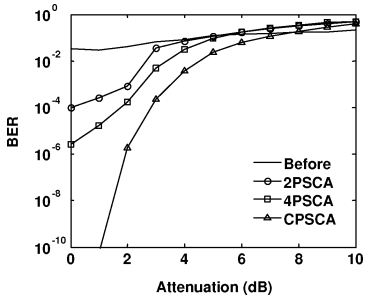

Fig. 6. Fiber configuration 4 μm/1000 m: BER versus attenuation before adaptation, and after CPSCA, 4PSCA, and 2PSCA.

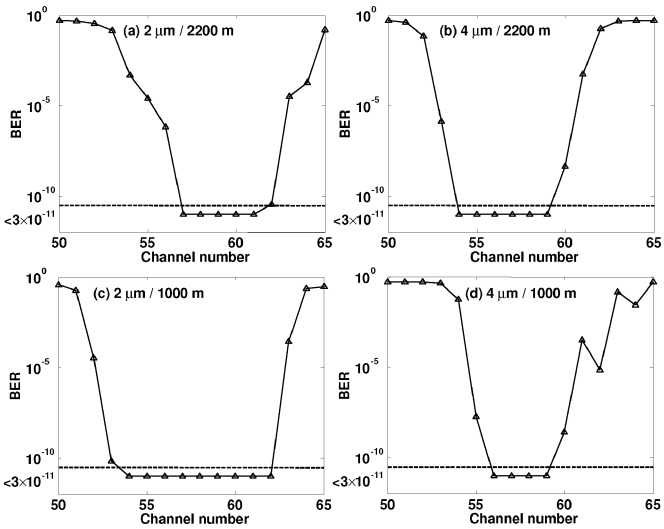

Fig. 7. BER versus channel number, after CPSCA. Fiber configurations: (a) 2 μm/2200 m, (b) 4 μm/2200 m, (c) 2 μm/1000 m, (d) 4 μm/1000 m. Channel spacing: 50 GHz. Channel 58 corresponds to 1550 nm, and is the channel used for adaptation.

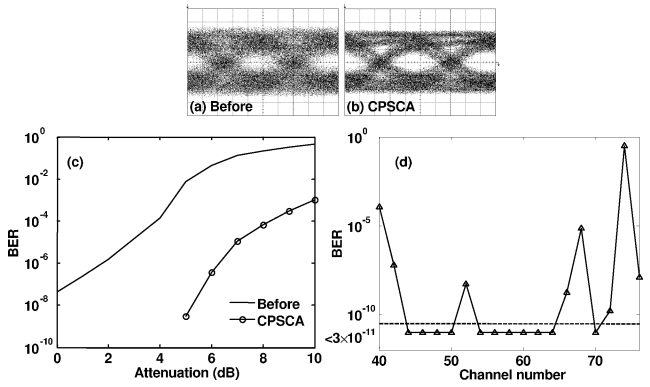

Fig. 8. Fiber configuration 0 μm/500 m/2 μm/500 m: eye diagrams (a) before adaptation, (b) after CPSCA; (c) BER versus attenuation; (d) BER versus channel number, after CPSCA; adaptation performed at channel 58.

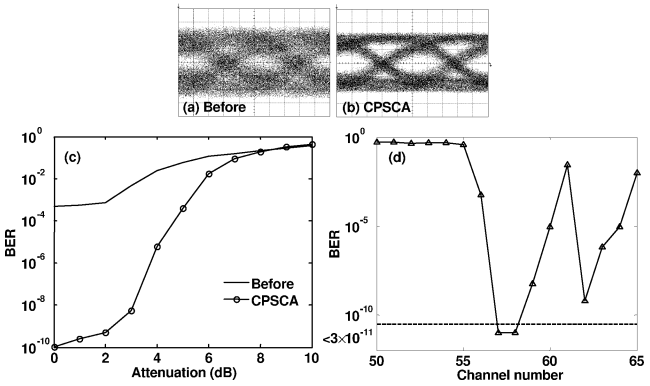

Fig. 9. Fiber configuration 0 μm/500 m/4 μm/500 m: eye diagrams (a) before adaptation, (b) after CPSCA; (c) BER versus attenuation; (d) BER versus channel number, after CPSCA; adaptation performed at channel 58.

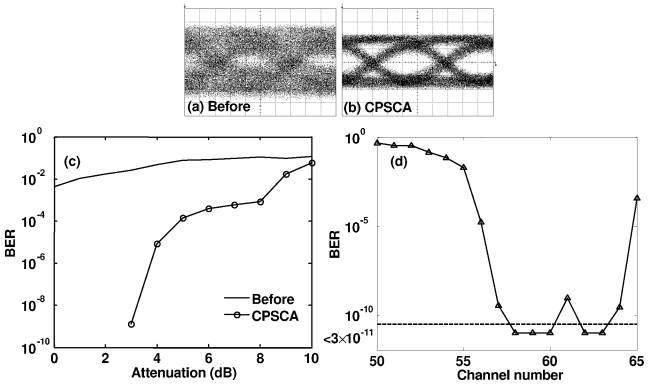

Fig. 10. Fiber configuration 2 μm/500 m/2 μm/500 m: eye diagrams (a) before adaptation, (b) after CPSCA; (c) BER versus attenuation; (d) BER versus channel number, after CPSCA; adaptation performed at channel 58.

focus on CPSCA. We first study the bandwidth characteristics of CPSCA, and then study the performance of CPSCA in the presence of midspan offset splices.

We first study the bandwidth range over which a single SLM, after adaptation using CPSCA, can compensate modal dispersion. This data is shown in Fig. 7(a)–(d) for the same four fiber configurations studied in Figs. 3–6. The laser frequency is switched over 50-GHz steps while holding the post-adaptation SLM pattern constant. Channel 58 corresponds to a wavelength of 1550 nm. These figures indicate that a single SLM pattern is able to compensate over multiple wavelengths, though the actual wavelength range compensated depends on the nature of the impairment.

Figs. 8–10 show the performance of CPSCA with three other fiber configurations. We have repeated each of these experiments several times, and have presented typical data sets from these experiments. These clearly demonstrate that CPSCA can compensate for modal dispersion in a wide range of fiber configurations, and over multiple wavelengths.

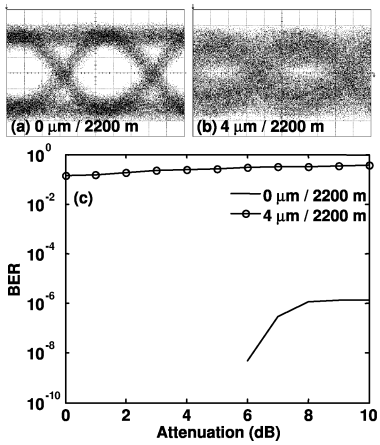

Fig. 11. Performance of fusion-spliced SMF-MMF patchcord, instead of adaptive optics system, in presence of offset patchcord. Eye diagrams (a) without offset patchcord, 0 μm/2200 m, and (b) with offset patchcord, 4 μm/2200 m; (c) BER versus attenuation.

An iteration of CPSCA over the entire SLM takes about 3 minutes in our lab setup. Therefore, when adaptation was attempted using fiber spans longer than 2.2 km, fiber drift occurred at time scales comparable to adaptation time. As discussed in Section III.D, dedicated hardware could reduce adaptation time to the order of 5.4 ms, which is significantly shorter than the time scales over which fiber drift occurs.

C. Comparison With Center Launch Using Fusion-Spliced SMF-MMF Patchcord

It was reported in [12] that modal dispersion compensation in MMF systems could be achieved by center-launching using a fusion-spliced SMF-MMF patchcord. We investigated the ability of this technique to compensate the effect of midspan offsets. The adaptive-optics setup was replaced by a fusion-spliced SMF-MMF patchcord, made with a recipe obtained from the authors of [12]. The launched power level was set to be equal to that in the adaptive transmission scheme. Fig. 11 shows eye patterns and BER curves with and without offset patchcords. While SMF-MMF patchcord is able to give error-free transmission in a link without offset impairments, it fails when an offset is introduced. This is because, while fusion splicing ensures a low-order mode launch because of good mode matching between the SMF and MMF, a low-order launch is not sufficient to compensate midspan offsets. Our adaptive optics approach can, however, compensate for modal dispersion in this offset-impaired fiber configuration.

V. Conclusion

We have experimentally compared various adaptive algorithms for compensation of modal dispersion in MMF using an SLM, and have shown that CPSCA gives better BER performance than 2PSCA or 4PSCA. We have shown that multiple 10-Gb/s channels, spaced by 50 GHz, can be compensated by a single SLM adapted using CPSCA, demonstrating its possible use in WDM transmission. We have also shown that CPSCA is able to compensate for modal dispersion over up to 2.2 km, even in the presence of midspan offsets up to 4 μm.

Acknowledgment

The authors would like thank A. Singh Saluja for his help in implementing portions of the LabView code used in the experiments.

References

[1] G. P. Agrawal, *Fiber-Optic Communications Systems*, 3rd ed. New York: Wiley, 2002.
[2] S. Fan and J. M. Kahn, "Principal modes in multi-mode waveguides," *Opt. Lett.*, vol. 30, no. 2, pp. 135–137, Jan. 2005.
[3] X. Zhao and F. S. Choa, "Demonstration of 10-Gb/s transmissions over 1.5-km-long multimode fiber using equalization techniques," *IEEE Photon. Technol. Lett.*, vol. 14, no. 8, pp. 1187–1189, Aug. 2002.
[4] H. Wu, J. A. Tierno, P. Pepeljugoski, J. Schaub, S. Gowda, J. A. Kash, and A. Hajimiri, "Integrated transversal equalizers in high-speed fiber-optic systems," *IEEE J. Solid-State Circuits*, vol. 38, pp. 2131–2137, Dec. 2003.
[5] J. G. Proakis, *Digital Communications*, 4th ed. New York: McGraw-Hill, 2001.
[6] E. Alon, V. Stojanovic, J. M. Kahn, S. P. Boyd, and M. A. Horowitz, "Equalization of modal dispersion in multimode fiber using spatial light modulators," in *Proc. Global Telecommun. Conf.*, Dallas, TX, Nov. 2004, pp. 1023–1029.
[7] R. A. Panicker, J. M. Kahn, and S. P. Boyd, "Compensation of multimode fiber dispersion using adaptive optics via convex optimization," *J. Lightw. Technol.*, vol. 26, no. 10, p. 1295–1305, May 2008.
[8] X. Shen, J. M. Kahn, and M. A. Horowitz, "Compensation for multimode fiber dispersion by adaptive optics," *Opt. Lett.*, vol. 30, no. 22, pp. 2985–2987, Nov. 2005.
[9] R. A. Panicker, J. P. Wilde, J. M. Kahn, D. F. Welch, and I. Lyubomirsky, "10×10 Gb/s DWDM transmission through 2.2 km multimode fiber using adaptive optics," *IEEE Photon. Technol. Lett.*, vol. 19, no. 15, pp. 1154–1156, Aug. 2007.
[10] R. A. Panicker and J. M. Kahn, "Algorithms for compensation of multimode fiber dispersion using adaptive optics," *J. Lightw. Technol.*, Nov. 2007, to be published.
[11] S. Cornelissen, T. G. Bifano, and P. A. Bierden, "MEMS spatial light modulators with integrated electronics," *Proc. SPIE*, vol. 4561, pp. 28–34, 2001.
[12] D. H. Sim, Y. Takushima, and Y. C. Chung, "Transmission of 10-Gb/s and 40-Gb/s signals over 3.7 km of multimode miber using mode-field matched center launching technique," in *Proc. OFC/NFOEC 2007*, Mar. 25–29, 2007, Paper OTuL3.

Rahul Alex Panicker received the B.Tech. degree from the Indian Institute of Technology (IIT), Madras, India, in 2002, and the M.S. and Ph.D. degrees from Stanford University, Stanford, CA, in 2004 and 2007, respectively, all in electrical engineering.

He spent 2008 working with the Optical Systems Group at Infinera Corporation. His research interests included applying convex-optimization techniques to optical communications systems and designing next-generation systems based on Infinera's photonic-integrated-circuit technology. He currently works as President of Rural Products at Embrace, Bangalore, India, a company trying to save premature babies in developing countries through a low-cost infant warmer that can work without electricity.

Alan Pak Tao Lau received the B.A.Sc. degree in engineering science (electrical option) and the M.A.Sc. degree in electrical and computer engineering from the University of Toronto, Toronto, ON, Canada, in 2003 and 2004, respectively. He then received the Ph.D. degree in electrical engineering from Stanford University, Stanford, CA, in 2008 in coherent optical communications.

He also worked at NEC Labs America in 2006 as a research associate in the Optical Networking Division. He is the recipient of numerous government awards during his post-graduate study at Stanford University and University of Toronto. His current research interests include system design, signal processing and performance monitoring techniques for coherent optical communication systems. He is currently an Assistant Professor in the Electrical Engineering Department of the Hong Kong Polytechnic University.

Dr. Lau is a member of OSA and serves as a reviewer and technical program committee member for numerous international journals and conferences in the area of photonics and communications.

Jeffrey P. Wilde received the M.S. and Ph.D. degrees in applied physics from Stanford University, Stanford, CA, in 1989 and 1992, respectively. His thesis work involved the growth and characterization of photorefractive crystals for multiplex holography.

He has co-founded three companies having core technologies centered around optics and photonics. In 1994 he started 3D Technology Labs to pursue materials development for holographic data storage. In 1996 he co-founded Quinta Corporation, a data storage company based on a new type of high-capacity magneto-optic disk drive technology that utilized flying optical heads with single-mode fiber for light transmission and MEMS mirrors for high-bandwidth track following. Quinta was acquired by Seagate Technology in 1997, and he subsequently served as Director of Research West for Seagate. He left Seagate in 2000 and started Capella Photonics to develop wavelength switching technology for the optical telecommunications industry. Capella offers reconfigurable optical add-drop products for both metro and long-haul applications. Since 2003, he has served as a consultant and advisor to various start-up companies. He is currently a visiting scholar in the Electrical Engineering Department at Stanford University, where he is working on high-speed fiber communication technology.

Dr. Wilde is a member of the Institute of Electronics and Electrical Engineers and the Optical Society of America.

Joseph M. Kahn (M'90–SM'98–F'00) received the B.A., M.A., and Ph.D. degrees in physics from the University of California at Berkeley in 1981, 1983, and 1986, respectively.

From 1987-1990, he was at AT&T Bell Laboratories, Crawford Hill Laboratory, Holmdel, NJ. He demonstrated multi-Gb/s coherent optical fiber transmission systems, setting world records for receiver sensitivity. From 1990-2003, he was on the faculty of the Department of Electrical Engineering and Computer Sciences at U.C. Berkeley, performing research on optical and wireless communications. Since 2003, he has been a Professor of Electrical Engineering at Stanford University. His current research interests include single- and multi-mode optical fiber communications, free-space optical communications, and MEMS for optical communications.

Prof. Kahn received the National Science Foundation Presidential Young Investigator Award in 1991. From 1993-2000, he served as a Technical Editor of IEEE *Personal Communications Magazine*. Since 2009, he has been an Associate Editor of IEEE/OSA JOURNAL OF OPTICAL COMMUNICATIONS AND NETWORKING. In 2000, he helped found StrataLight Communications (now Opnext Subsystems), where he served as Chief Scientist from 2000-2003.